Electron Diffusion Length in Mesoporous Nanocrystalline TiO2 Photoelectrodes during Water Oxidation

ARTICLE *in* JOURNAL OF PHYSICAL CHEMISTRY LETTERS · FEBRUARY 2010

Impact Factor: 7.46 · DOI: 10.1021/jz100051q

5 AUTHORS, INCLUDING:

Piers R. F. Barnes
Imperial College London
79 PUBLICATIONS **3,486** CITATIONS

SEE PROFILE

THE JOURNAL OF PHYSICAL CHEMISTRY Letters

pubs.acs.org/JPCL

Electron Diffusion Length in Mesoporous Nanocrystalline TiO_2 Photoelectrodes during Water Oxidation

W. H. Leng,* Piers R. F. Barnes,* Mindaugas Juozapavicius, Brian C. O'Regan, and James R. Durrant

Department of Chemistry, Imperial College London, Exhibition Road, London SW7 2AZ

ABSTRACT A long electron diffusion length (L) relative to film thickness is required for efficient collection of charge in photoelectrodes. L was measured in a nanocrystalline, mesoporous TiO_2 electrode during photochemical water splitting by two independent methods: (1) analyzing the ratio of incident photon conversion efficiency (IPCE) measured under back and front side illumination, and (2) analyzing transient photovoltage rise and decay measurements. These gave values of L that agreed (L = 8.5−12.5 μm between −0.15 and 0.1 V vs Ag/AgCl 3 M KCl at pH 2). The transient measurements were consistent with trap limited transport and recombination of electrons as previously observed in dye-sensitized solar cells. $L \sim 10$ μm is sufficient to collect separated electrons with minor electrolyte recombination losses in thin electrodes. However, charge collection may limit performance in doped mesoporous electrodes with weak visible light absorption where thicker films are required.

SECTION Electron Transport, Optical and Electronic Devices, Hard Matter

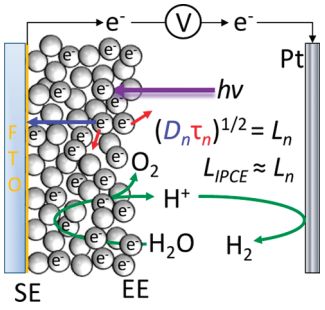

The direct splitting of water into hydrogen and oxygen using light in semiconducting photoelectrochemical (PEC) cells has received much attention since the concept was first demonstrated[1] because of hydrogen's potential as a fuel.[2,3] There have been extensive efforts to discover and design suitable photoelectrode materials for this process.[4−6] Although TiO_2 only absorbs light in the UV part of the solar spectrum, it remains of great interest as a model system due to its ease of preparation and operational stability,[7] as well as the possibility of reducing its band gap.[6] Additionally, since the successful application of nanocrystalline TiO_2 in dye-sensitized solar cells (DSSCs), creating a bulk heterojunction, the use of mesoporous photoelectrodes appears to be an interesting alternative to bulk electrodes for PEC water splitting.[8] The photoelectrode structure must facilitate the spatial separation of the water oxidation process using photogenerated holes at the TiO_2 surface and the reduction process using photogenerated electrons to form hydrogen at the cell counter electrode. For such photoreactors, efficient collection of electrons through the nanocrystalline TiO_2 is important. Electron collection has been studied extensively in DSSCs where electron trapping has been shown to be important in determining the process dynamics. However, electron collection dynamics and diffusion length have received little attention in studies of water photooxidation.

It is not yet clear whether the benefits of nanostructuring electrodes outweigh the disadvantages. The advantages are the high surface area and absorption volume close to the semiconductor−electrolyte interface, allowing effective collection and reaction of photogenerated holes. The disadvantages are the partial loss of electric field for charge separation and the massively increased opportunity for electrons to recombine with species on the electrode surface or in the electrolyte before they are collected at the electrode substrate. In nanoporous TiO_2 electrodes, the high dielectric constant ($\varepsilon_r \sim 80-120$) and small size (~20 nm) of the nanocrystals mean that photogenerated charge carriers are thought to be screened from significant electric fields by the electrolyte so that transport of electrons is dominated by diffusion.[9−11]

The electron diffusion length, L, can be a useful parameter for describing the competition between the diffusive transport and recombination of charge carriers in a photoelectrode, and it forms the subject of this communication. It is defined most simply as the average displacement of an electron before recombination and, if first order recombination in electrons is obeyed, it can be written as (see Supporting Information)

$$L = (D_0\tau_0)^{1/2} \quad (1)$$

where D_0 is the conduction band electron diffusion coefficient, and τ_0 is the conduction band electron lifetime. The mechanism of electron recombination during the photooxidation of water is not fully understood. There are a number of possible electron acceptor species: electrons could recombine with relatively immobile photogenerated species such as trapped holes or surface-bound hydroxyl radicals, and/or species more evenly distributed such as photooxidation reaction intermediates (e.g., peroxo species) or products such as

Received Date: January 14, 2010
Accepted Date: February 22, 2010
Published on Web Date: February 26, 2010

DOI: 10.1021/jz100051q | *J. Phys. Chem. Lett.* **2010**, *1*, 967–972

oxygen. In this work we apply the simplest possible model of recombination that has been successfully applied to understand the behavior of DSSCs, namely, that there is an approximately homogeneous distribution of electron accepting species in solution or on the photoelectrode surface with an approximately constant recombination time constant τ_0 as discussed below. L has not yet been determined in nanoporous TiO_2 photoelectrodes during the photooxidation of water; here we demonstrate two independent approaches for estimating L. As recently emphasized by Bisquert et al.,[12,13] and modeling work of Villanueva-Cab et al.,[14] if the order of electron recombination is sublinear, then τ_0 is not constant, and L can only be defined for the small perturbation limit where the electron concentration is approximately constant within a device. Both the techniques described in this work are small perturbation measurements, i.e., the measurements are made with an approximately constant background electron concentration with a small additional electron concentration. These approaches allow us to test whether water splitting photoelectrodes can be understood in terms of behavior observed in DSSCs: transport and recombination dominated by a small fraction of electrons in the conduction band, which are in dynamic equilibrium with the majority of electrons localized within an exponential distribution of trap states below the conduction band. This description is sometimes referred to as the multiple trapping model with the quasi-static approximation.[15]

Lindquist et al. originally developed a model for analysis of the incident photon conversion efficiency (IPCE; which we write as η_{IPCE}) of microporous semiconductor films in PEC cells based on a constant τ_0 from which L could be derived from measurements with illumination from the substrate−electrode (SE) side versus the electrolyte−electrode (EE) side.[9] Notwithstanding theoretical questions regarding the derivation of L, SE and EE IPCE measurements can unambiguously show whether electrons can be collected across the entire film thickness. L is just one method of quantifying this observable. We use their approach and include a charge separation efficiency (η_{sep}) analogous to the analysis for DSSCs,[16,17] which could be interpreted in terms of recombination to localized photogenerated species. Thus, in one dimension at steady state where trapped electrons are in balance with conduction electrons, the excess concentration of conducting electrons (n_c) as a function of position (x) in the electrode can be described by[17]

$$D_0 \frac{\partial^2 n_c(x)}{\partial x^2} - \frac{n_c(x) - n_{c0}(0)}{\tau_0} + \eta_{sep} G(x) = 0 \qquad (2)$$

where n_{c0} is the dark conduction electron concentration at the potential held by the potentiostat, and $G(x)$ is the generation rate of electron hole pairs with illumination from the EE or SE side approximated by

$$G_{EE}(x) = (1 - R_{EE})\alpha\Phi_0 e^{-\alpha x} \qquad (3)$$

$$G_{SE}(x) = (1 - R_{SE})\alpha\Phi_0 e^{-\alpha x} \qquad (4)$$

R_{EE} and R_{SE} are the reflectance of each side of the photoelectrode with film thickness d and TiO_2 absorption coefficient α, and $x = 0$ is the start of the illuminated side. Equations 2 and 3 or 4 can be solved to derive expressions for the IPCE for either EE or SE side illumination (see Section 3, Supporting Information). Given eq 1, the ratio of $\eta_{IPCE,\,EE}/\eta_{IPCE,\,SE}$ can then be written as expression 5, which is dependent only on L, R, d, and α.

$$\frac{\eta_{IPCE,EE}}{\eta_{IPCE,SE}} = \frac{(1 - R_{EE})[(L\alpha + 1)e^{2d/L} - 2L\alpha e^{\alpha d + d/L} + L\alpha - 1]}{(1 - R_{SE})[(L\alpha + 1)e^{\alpha d + 2d/L} + (L\alpha + 1)e^{\alpha d} - 2L\alpha e^{d/L}]} \qquad (5)$$

Since R, d, and α can be measured independently, L can be found with a single parameter fit to the ratio of EE to SE side IPCE data.

We have also used small perturbation photovoltage transient (TPV) measurements of the effective diffusion coefficient and recombination lifetime (D_n) and (τ_n) to find L. Photovoltage rise measurements are useful, avoiding the RC limitations of photocurrent transient measurements at high electron concentrations.[18] The data we present suggests that the multiple trapping model with first-order electron recombination gives a valid description of the photoelectrode so that the quasi-static approximation can be used to write $L = (D_0\tau_0)^{1/2} = (D_n\tau_n)^{1/2}$.[15,17] Using a modification of our previous method,[18] the single exponential part of the photovoltage rise after a short, uniformly generating, illumination pulse has a time constant τ_{rise}, which can be related to D_n by

$$D_n = \frac{d^2}{\pi^2}\left(1 + \frac{3}{1 + \left(\frac{3}{\sqrt{2}} - 1\right)\frac{C_{TiO2}}{C_{sub}}}\right)\left(\frac{1}{\tau_{rise}} - \frac{1}{\tau_n}\right) \qquad (6)$$

where C_{TiO2} and C_{sub} are the differential capacitance of TiO_2 and the capacitance of the conducting substrate at a given potential, respectively. Equation 6 indicates that the relationship between D_n and τ_{rise} varies between two limiting situations: the case where C_{sub} is negligible relative to C_{TiO2} and the situation where C_{TiO2} is negligible relative to C_{sub}, in which case τ_{rise} is identical to the transient photocurrent time constant. The origin of the expression is described in detail in section 4 of the Supporting Information. It follows from eq 6 that D_n can be determined from τ_{rise} and τ_n if C_{TiO2} and C_{sub} are also measured. The time constant for the single exponential decay component of the TPV gives the effective electron lifetime (τ_n), allowing L to be found.

We now demonstrate the applicability of these two techniques on a TiO_2 water splitting system. Figure 1a shows examples of the IPCE measured on a nanocrystalline TiO_2 photoelectrode (d = 12.9 μm) at an applied potential of 0.0 V vs Ag/AgCl using EE and SE side illumination. It is apparent that electrons are poorly collected from the EE side of the film. Figure 1b shows the ratio of these measurements $\eta_{IPCE,\,EE}/\eta_{IPCE,\,SE}$ plotted against wavelength. The fit to this ratio data is also shown, which corresponds to a diffusion length L = 9.9 μm (for α, see Figure S8 in the Supporting Information). The fit to the data is reasonable, and the uncertainty of the fitted value of L is ~10% (at the 95% confidence level) if the simple model is correct. Also shown in Figure 1b are values of

DOI: 10.1021/jz100051q | J. Phys. Chem. Lett. 2010, 1, 967–972

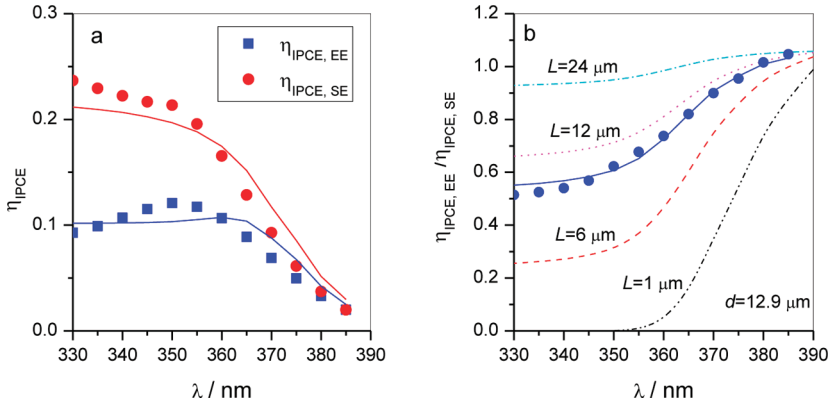

Figure 1. (a) Example of IPCE data for EE (squares, $\eta_{IPCE, EE}$) and SE (circles, $\eta_{IPCE, SE}$) side illumination under bias potential 0 V vs Ag/AgCl in 0.5 M $NaClO_4$ aqueous solutions (pH = 2.0). Also shown are the fits to the data using L derived in panel b, where $\eta_{sep} = 0.25$. (b) Calculated wavelength-dependent $\eta_{IPCE, EE}/\eta_{IPCE, SE}$ as a function of electron diffusion length L and example of fit to the $\eta_{IPCE, EE}/\eta_{IPCE, SE}$ data where $L = 9.9$ μm.

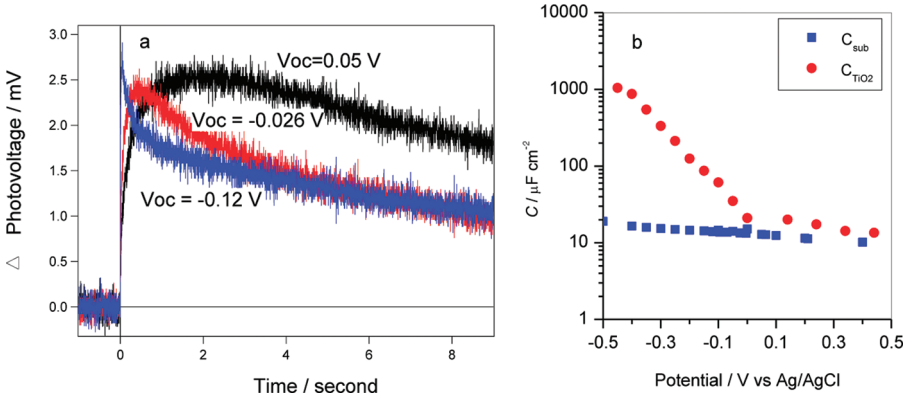

Figure 2. (a) Examples of transient photovoltage vs time at varying bias light controlled V_{oc}'s. (b) Capacitance of the nc-TiO_2 electrode as a function of potential (determined by chronoamperometry in the dark). The capacitance of the FTO substrate is also shown (determined by impedance measurements, see Experimental Section).

$\eta_{IPCE, EE}/\eta_{IPCE, SE}$ calculated with a range of different diffusion lengths. The calculated curves show that a longer L leads to higher IPCE ratios, particularly at short wavelengths where α is large. As expected, if L becomes comparable to or larger than d, most of the photogenerated electrons are collected before they are able to recombine, regardless of the illumination side (see also Figure S9 in the Supporting Information). If $L \ll d$, then most electrons generated far from the collecting electrode will recombine, resulting in a low EE/SE side IPCE ratio (Figure S9). When $L > d$, the method becomes progressively less sensitive, leading to uncertainty in the estimation of L as was discussed by Wang et al. in their study of water photooxidation using nanoporus WO_3 films.[19] Figure 1a also shows fits to $\eta_{IPCE, EE}$ and $\eta_{IPCE, SE}$ using the value of L derived in Figure 1b, which allows the charge separation efficiency η_{sep} to be estimated, as will be reported in detail in a separate study.

Figure 2a shows examples of TPV versus time at different open circuit potentials controlled by varying bias light intensities. The transients show a photovoltage rise, which can be described by a single exponential (τ_{rise}) and biphasic photovoltage decay with a single exponential initial phase and a long tail (the origin of the tail may be related to slow H^+ intercalation as has been discussed previously for both Li^+ and H^+[20]). For this study we used the initial phase to determine τ_n. Figure 2b shows that the capacitance of the fluorine-doped tin oxide (FTO) substrate is almost independent of applied potential, while C_{TiO2} versus potential exhibits an exponential relationship, consistent with an exponential distribution of localized trapping states below the TiO_2 conduction band edge, as is well documented in DSSCs.[15] The potential dependence of τ_{rise} and τ_n is shown in Figure 3a. Both parameters decreased exponentially with decreasing potential (increasing light intensity). This decreasing trend in τ_{rise} corresponds to an increase in D_n (calculated using the capacitance data in Figure 2b and eq 6). This can be interpreted as being due to an increasing ratio of conducting to trapped electrons as the Fermi level (and the total concentration of electrons) in the film increases (c.f. the C_{TiO2} measurements in Figure 2b). Similarly, the decrease in τ_n can be explained by recombination being proportional to the fraction of conducting electrons, which increases as the Fermi level rises. The values of D_n observed in Figure 3a are approximately one order in magnitude smaller than those

DOI: 10.1021/jz100051q | J. Phys. Chem. Lett. 2010, 1, 967–972

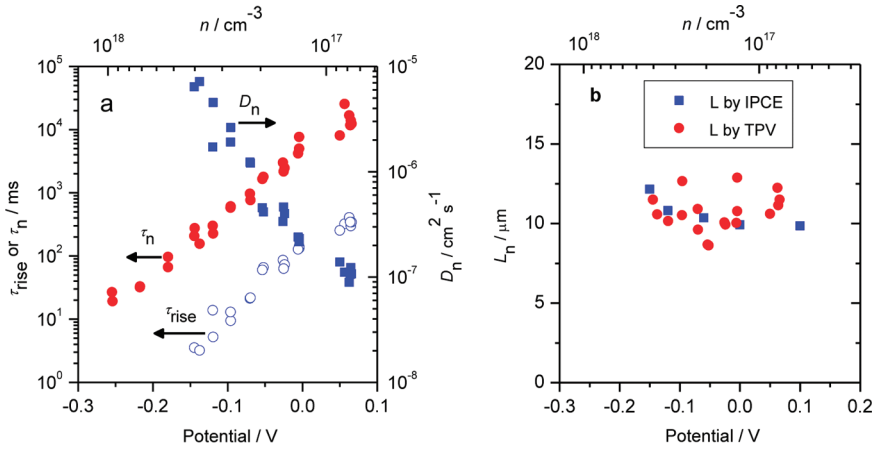

Figure 3. (a) Dependence of photovoltage rise time (τ_{rise}) effective electron lifetime (τ_n) and effective electron diffusion coefficient D_n on dc photovoltage/electron density. (b) Comparison of electron diffusion lengths derived from the IPCE measurements and from the transient measurements as a function of potential (note that the open potential in the dark was +0.21 V vs Ag/AgCl).

in our previous DSSC studies.[17] The reason for this variation may be related to the difference in solvent impeding the movement of electrons, as we have observed similarly low diffusion coefficients in DSSCs containing aqueous electrolyte.

Figure 3b shows values of the diffusion length determined using pairs of D_n and τ_n values determined by the TPV method together with those values derived by IPCE measurements at different potentials and electron concentrations. Despite the uncertainty in interpreting the biphasic the photovoltage decays and what is probably an oversimplified model of the IPCE, the two different methods give remarkably similar and constant results over the potential range studied. This is particularly notable given the difference in experimental techniques—low light intensity steady-state photocurrent at fixed potentials versus small transient photovoltage measurements at open circuit. In contrast, studies on DSSCs indicate a 2−3-fold difference between transient and steady-state measurements of apparent L, and L is also typically a function of electron concentration.[17,21,22] This may be related to differing orders of transport and recombination kinetics for electrons in DSSCs.[12,23] In our present results, L is relatively independent of potential (electron concentration), implying first-order recombination kinetics with electrons. Consequently, the two methodologies should agree, as is observed. This suggests that, to a first approximation, the electron transport model we have employed (including the transient effects of multiple trapping) may provide an adequate description of photoelectrode behavior during water splitting. Note that the measured L in water is much smaller than that reported in aqueous solutions with efficient organic holes scavengers (up to 400 μm),[24] further suggesting that electrons can recombine with hole species during collection. Still, in our case the film thickness required to harvest the majority of incident light in the UV part of the spectrum is still less than the diffusion length ($d < L \approx 10$ μm, $\alpha(370\text{ nm})^{-1} \approx 10$ μm, such that $\eta_{col} > \sim 0.8$; see Figures S8a and S9), thus electron collection will not be the primary factor limiting IPCE in nanocrystalline TiO_2 electrodes optimized for UV light. However, efforts to reduce the band gap of TiO_2, for example, by N doping,[6] typically show a large absorption depth (α^{-1}) in the visible region, thus requiring large film thicknesses for effective light harvesting; in this circumstance electron collection is a potentially significant limiting factor.

In summary we have demonstrated that diffusion lengths can be measured by two independent methods on a water splitting system. The quantitative agreement between the techniques using IPCE and transient photovoltage rise and decay times suggests a simple model of electron transport, and recombination may give a reasonable approximation of the electron loss during transport in a nanoporus water splitting electrode. The transient measurements also show that the multiple trapping model gives a valid description of electron behavior during the photooxidation of water. The measured values of L (8.5−12.5 μm) are sufficient to allow the efficient collection of electrons in electrodes optimized to harvest UV light, and efforts to improve this electrode performance should thus concentrate on the charge separation efficiency. However, longer electron diffusion lengths may be required for doped nanocrystalline TiO_2.

EXPERIMENTAL SECTION

All reagents were of at least analytical grade and used as received from Sigma Aldrich. $NaClO_4$ electrolyte solutions (0.5 M) with pH 2 adjusted by $HClO_4$ (99.999%) were prepared from Milli-Q water (Millipore Corp, 18.2 MΩ cm at 25 °C, DI). Nanocrystalline TiO_2 films were prepared on conductive fluorine doped glass (FTO) by a doctor blade method.[25] TiO_2 films were also prepared on a coverslip (50 μm thick) for optical measurements by the same method. The film thickness was measured using a profilometer (Alpha-Step 200, Tencor Instruments). To make a photoelectrode, an electrical contact was made with FTO substrate by using silver conducting paste connected to a copper wire. The working geometric surface area of TiO_2 was 1.0 × 1.0 cm^2 with the remainder covered by one-component silicone adhesive (Dow Corning 732). The electrodes were thoroughly washed with deionized (DI) water before use.

DOI: 10.1021/jz100051q | J. Phys. Chem. Lett. 2010, 1, 967–972

The transmittance measurements for a PEC cell with the electrolyte were made with a Shimadzu UV−vis dual beam Spectrophotometer (UV-1601). The transmittance and reflectance measurements, both for samples and for substrate, were made with a spectrophotometer (Lambda 950, PerkinElmer) equipped with an integrating sphere. These measurements were carried out for wet films penetrated with the electrolyte. No obvious difference in transmittance for the TiO_2 samples between these measurements and those measured in the cuvet with the electrolyte was found.

IPCE experiments were performed in a PEC cell with two quartz windows using a 75 W xenon bulb (Ushio, with PTI stabilized current power supply) as the illumination source coupled with a monochromator (MD-1000, 1200 g/mm blaze 400 nm, Optical Building Blocks Corp. Birmingham). The working electrode was the TiO_2 electrode (illumination area about 0.6×0.6 cm^2), illuminated from either the SE side or the TiO_2 EE side. Platinum gauze (99.9%) was used as the counter electrode, and a 3 M KCl Ag/AgCl electrode (SSE, Bioanalytical Systems Ltd.) was used as the reference electrode. All the potentials in the paper will be referred to SSE at 25 °C. Oxygen-free nitrogen gas was bubbled through the electrolyte before and during the experiments. The intensity of the incident light was measured with an optical power meter (PM120 V, Thorlabs) equipped with a UV sensor (model S120UV, Thorlabs). Applied potentials were controlled by a commercial computer-controlled potentiostat (Autolab 12). The photocurrent was defined as the difference in current between illuminated and dark conditions measured after illuminating for 1 min.

Transient photovoltages were taken with the use of a pump pulse generated by UV light-emitting diodes (LEDs, OTLH-0480-UV, 365 ± 10 nm, Opto Technology, Inc.) controlled by a fast solid-state switch. UV bias light was supplied by another array of the same LEDs, and the light intensity was modulated by varying the current supplied to the LEDs. The pulse was incident on the EE side of the photoelectrode. Pulse intensity was adjusted to maintain the amplitude of the transient photovoltage below 5 mV. Transients were measured using National Instruments USB-6211 multifunction data acquisition box interfaced to a PC. No signal averaging was required. Both the photovoltage rise and decay time constants were determined by fitting single exponentials.

The capacitance of TiO_2 and the FTO substrate was measured by chronoamperometry and impedance measurements, respectively.

All the experiments were conducted at room temperature (25 °C). All experiments were repeated at least twice. Further details can be found in the Supporting Information.

SUPPORTING INFORMATION AVAILABLE

Experimental and analytical details. This material is available free of charge via the Internet at http://pubs.acs.org.

AUTHOR INFORMATION

Corresponding Author:

*To whom correspondence should be addressed. E-mail: w.leng@imperial.ac.uk (W.H.L.); piers.barnes@imperial.ac.uk (P.R.F.B.).

ACKNOWLEDGMENT

This work was funded by the EPSRC. We are grateful to Li Xiaoe for the TiO_2 paste preparation, to Assaf Anderson for his insights and development of the experimental equipment, and to Junwang Tang, Alexander Cowan, Stephanie Pendlebury, and Stephen Dennison for useful discussions.

REFERENCES

(1) Fujishima, A.; Honda, K. Electrochemical Photolysis of Water at a Semiconductor Electrode. *Nature* **1972,** *238*, 37–38.

(2) Turner, J. A. Sustainable Hydrogen Production. *Science* **2004,** *305*, 972–974.

(3) Esswein, M. J.; Nocera, D. G. Hydrogen Production by Molecular Photocatalysis. *Chem. Rev.* **2007,** *107*, 4022–4047.

(4) Kay, A.; Cesar, I.; Gratzel, M. New Benchmark for Water Photooxidation by Nanostructured α-Fe_2O_3 films. *J. Am. Chem. Soc.* **2006,** *128*, 15714–15721.

(5) Osterloh, F. E. Inorganic Materials as Catalysts for Photochemical Splitting of Water. *Chem. Mater.* **2008,** *20*, 35–54.

(6) Asahi, R.; Morikawa, T.; Ohwaki, T.; Aoki, K.; Taga, Y. Visible-Light Photocatalysis in Nitrogen-Doped Titanium Oxides. *Science* **2001,** *293*, 269–271.

(7) Hoffmann, M. R.; Martin, S. T.; Choi, W.; Bahnemann, D. W. Environmental Applications of Semiconductor Photocatalysis. *Chem. Rev.* **1995,** *95*, 69–96.

(8) Mor, G. K.; Varghese, O. K.; Paulose, M.; Shankar, K.; Grimes, C. A. A Review on Highly Ordered, Vertically Oriented TiO_2 Nanotube Arrays: Fabrication, Material Properties, and Solar Energy Applications. *Sol. Energy Mater. Sol. Cells* **2006,** *90*, 2011–2075.

(9) Sodergren, S.; Hagfeldt, A.; Olsson, J.; Lindquist, S. E. Theoretical-Models for the Action Spectrum and the Current−Voltage Characteristics of Microporous Semiconductor Films in Photoelectrochemical Cells. *J. Phys. Chem.* **1994,** *98*, 5552–5556.

(10) O'Regan, B.; Moser, J.; Anderson, M.; Gratzel, M. Vectorial Electron Injection into Transparent Semiconductor Membranes and Electric-Field Effects on the Dynamics of Light-Induced Charge Separation. *J. Phys. Chem.* **1990,** *94*, 8720–8726.

(11) Nakade, S.; Saito, Y.; Kubo, W.; Kanzaki, T.; Kitamura, T.; Wada, Y.; Yanagida, S. Laser-Induced Photovoltage Transient Studies on Nanoporous TiO_2 Electrodes. *J. Phys. Chem. B* **2004,** *108*, 1628–1633.

(12) Bisquert, J.; Mora-Seró, I. Simulation of Steady-State Characteristics of Dye-Sensitized Solar Cells and the Interpretation of the Diffusion Length. *J. Phys. Chem. Lett.* **2009,** *1*, 450–456.

(13) Bisquert, J.; Fabregat-Santiago, F.; Mora-Seró, I.; Garcia-Belmonte, G.; Gimenez, S. Electron Lifetime in Dye-Sensitized Solar Cells: Theory and Interpretation of Measurements. *J. Phys. Chem. C* **2009,** *113*, 17278–17290.

(14) Villanueva-Cab, J.; Oskam, G.; Anta, J. A. A Simple Numerical Model for the Charge Transport and Recombination Properties of Dye-Sensitized Solar Cells: A Comparison of Transport-Limited and Transfer-Limited Recombination. *Sol. Energy Mater. Sol. Cells* **2010,** *94*, 45–50.

(15) Bisquert, J.; Vikhrenko, V. S. Interpretation of the Time Constants Measured by Kinetic Techniques in Nanostructured Semiconductor Electrodes and Dye-Sensitized Solar Cells. *J. Phys. Chem. B* **2004,** *108*, 2313–2322.

(16) Halme, J.; Boschloo, G.; Hagfeldt, A.; Lund, P. Spectral Characteristics of Light Harvesting, Electron Injection, and Steady-State Charge Collection in Pressed TiO_2 Dye Solar Cells. *J. Phys. Chem. C* **2008,** *112*, 5623–5637.

(17) Barnes, P. R. F.; Anderson, A. Y.; Koops, S. E.; Durrant, J. R.; O'Regan, B. C. Electron Injection Efficiency and Diffusion Length in Dye-Sensitized Solar Cells Derived from Incident Photon Conversion Efficiency Measurements. *J. Phys. Chem. C* **2009,** *113*, 1126–1136.
(18) O'Regan, B. C.; Bakker, K.; Kroeze, J.; Smit, H.; Sommeling, P.; Durrant, J. R. Measuring Charge Transport from Transient Photovoltage Rise Times. A New Tool To Investigate Electron Transport in Nanoparticle Films. *J. Phys. Chem. B* **2006,** *110*, 17155–17160.
(19) Wang, H.; Lindgren, T.; He, J.; Hagfeldt, A.; Lindquist, S.-E. Photolelectrochemistry of Nanostructured WO_3 Thin Film Electrodes for Water Oxidation: Mechanism of Electron Transport. *J. Phys. Chem. B* **2000,** *104*, 5686–5696.
(20) Willis, R. L.; Olson, C.; O'Regan, B.; Lutz, T.; Nelson, J.; Durrant, J. R. Electron Dynamics in Nanocrystalline ZnO and TiO_2 Films Probed by Potential Step Chronoamperometry and Transient Absorption Spectroscopy. *J. Phys. Chem. B* **2002,** *106*, 7605–7613.
(21) Barnes, P. R. F.; Liu, L.; Li, X.; Anderson, A. Y.; Kisserwan, H.; Ghaddar, T. H.; Durrant, J. R.; O'Regan, B. C. Re-evaluation of Recombination Losses in Dye-Sensitized Cells: The Failure of Dynamic Relaxation Methods to Correctly Predict Diffusion Length in Nanoporous Photoelectrodes. *Nano Lett.* **2009,** *9*, 3532–3538.
(22) Wang, H.; Peter, L. M. A Comparison of Different Methods To Determine the Electron Diffusion Length in Dye-Sensitized Solar Cells. *J. Phys. Chem. C* **2009,** *113*, 18125–18133.
(23) Villanueva-Cab, J.; Wang, H.; Oskam, G.; Peter, L. M. Electron Diffusion and Back Reaction in Dye-Sensitized Solar Cells: The Effect of Nonlinear Recombination Kinetics. *J. Phys. Chem. Lett.* **2010,** *1*, 748–751.
(24) Lana-Villarreal, T.; Monllor-Satoca, D.; Gomez, R.; Salvador, P. Determination of Electron Diffusion Lengths in Nanostructured Oxide Electrodes from Photopotential Maps Obtained with the Scanning Microscope for Semiconductor Characterization. *Electrochem. Commun.* **2006,** *8*, 1784–1790.
(25) Tang, J.; Durrant, J. R.; Klug, D. R. Mechanism of Photocatalytic Water Splitting in TiO_2. Reaction of Water with Photoholes, Importance of Charge Carrier Dynamics, and Evidence for Four-Hole Chemistry. *J. Am. Chem. Soc.* **2008,** *130*, 13885–13891.

DOI: 10.1021/jz100051q | *J. Phys. Chem. Lett.* **2010,** *1*, 967–972